Temperature-Dependent Ways of Proton Transfer—A Benchmark Study on Cyclic HF Oligomers

Thomas Loerting and Klaus R. Liedl*

Institute of General, Inorganic and Theoretical Chemistry, University of Innsbruck, Innrain 52a, A-6020 Innsbruck, Austria

Received: May 5, 1999; In Final Form: July 19, 1999

Taking the example of vibrational-assisted concerted proton exchange in cyclic $(HF)_n$ ($n = 4, 5$) oligomers, we demonstrate that proton transfer occurs in three different ways, depending on the temperature. At high temperatures (>400 K) mainly overbarrier transitions take place. To predict the reaction rate, the barrier height needs to be known, at least at chemical accuracy. At intermediate temperatures (200−400 K) additionally an accurate knowledge of the barrier width is important, as the protons mainly tunnel through the barrier near its top. The adiabatic tunneling correction can be used to predict reaction dynamics, as the vibrational state does not change during the reaction. At low temperatures (<200 K) the slow skeletal modes are frozen and only fast hydrogenic movement takes place. For this reason vibrational adiabaticity is lost and a much wider region of the potential surface called reaction swath is crossed during the reaction. Predictions of the resulting exchange dynamics require the potential on the swath to be calculated accurately. In the zero-temperature limit these nonadiabatic tunneling paths solely determine the exchange reaction and cause spectroscopically measurable tunneling splittings, which can, therefore, be estimated reliably in the framework of transition-state theory from accurate calculations of energies on the reaction swath. All the above findings arise just from the fact that a light atom is transferred between two heavy atoms. Therefore, two crossover temperatures of proton transfer should qualitatively exist in all systems containing hydrogen bonds.

1. Introduction

In the Born−Oppenheimer approximation reaction dynamics is described by the underlying potential energy surface (PES).[1−5] Intramolecular proton-transfer reactions correspond to a special type of hypersurfaces as a result of the heavy−light−heavy mass combination of the nuclei involved.[6] This combination causes the entrance and the exit channels of the reaction to be at a very low skew angle.[7] A direct geometrical consequence of the shape of the surface is that both minima are spatially quite close to each other. A reaction path not crossing the transition state (TS) but alternatively directly connecting educt and product is therefore much shorter than the minimum energy path (MEP). However, it is also associated with a much higher barrier. As a result, the path selected is the best compromise between short and energetically low paths, the so-called least-action or instanton path.[6,8] This least-action path strongly depends on the temperature. At high temperatures the thermally available energy is sufficient to allow long paths, whereas at low temperatures shorter paths are taken, especially because tunneling reduces the energy requirement for the transition from one reaction well to the other. The regions along this least-action path comprise the MEP[2,7] and the reaction swath.[2,9,10] Statistical methods like transition-state theory (TST)[11,12] calculating thermally averaged reaction rate constants over all paths need a considerable number of points on this hypersurface to be calculated. An important question is the accuracy, i.e., the amount of computation time, needed to solve the electronic Schrödinger equation on these points. In Truhlar's group the microcanonical optimized multidimensional tunneling (μOMT)[9] method has been established. It yields accurate results for proton-transfer reaction rates, as it takes the maximum rate constant obtained from following two different reaction paths, namely, adiabatic paths in the region around the MEP and straight-line paths directly connecting both minima. In this work we present a benchmark calculation on the concerted proton exchange in cyclic $(HF)_n$ ($n = 4, 5$) oligomers as easy-to-handle prototype systems based on a complete *ab initio* hypersurface. We analyze the resulting dynamics predictions, i.e., reaction rate constants and spectroscopic tunneling splittings, on this hypersurface in comparison with the ones resulting from a recently presented surface relying on a specially parametrized semiempirical hypersurface.[13] Consequently, we gain a temperature-dependent picture of proton transfer in hydrogen bonds, presumably also valid for all other systems exhibiting proton transfer.

2. Methods

Canonical reaction rate constants were calculated from TST[7,14−19] (one of many reaction path methods applied currently to dynamics[20−32]) as implemented in POLYRATE8.0[33] utilizing the reaction path that follows the lowest energy part on the PES, i.e., the MEP. The MEP branches leading to both minima were generated by GAUSSIAN98[34] in combination with GAUSSRATE8.0[35] as the steepest-descent paths using the Page−McIver integrator.[36,37] For the description of corner cutting and tunneling semiclassical correction factors κ were applied. Namely, we used two different corrections: On the one hand, the small-curvature tunneling (SCT) correction,[38−40] which corresponds to the case of the adiabatic transition, where the tunneling path is at the concave side turning points of the harmonic oscillators along the MEP (i.e., the vibrational state does not change during the reaction). This correction is simply described by a reduction of the tunneling mass to an effective value gained from the

* To whom correspondence should be addressed.

10.1021/jp9914774 CCC: $18.00
Published on Web 10/22/1999

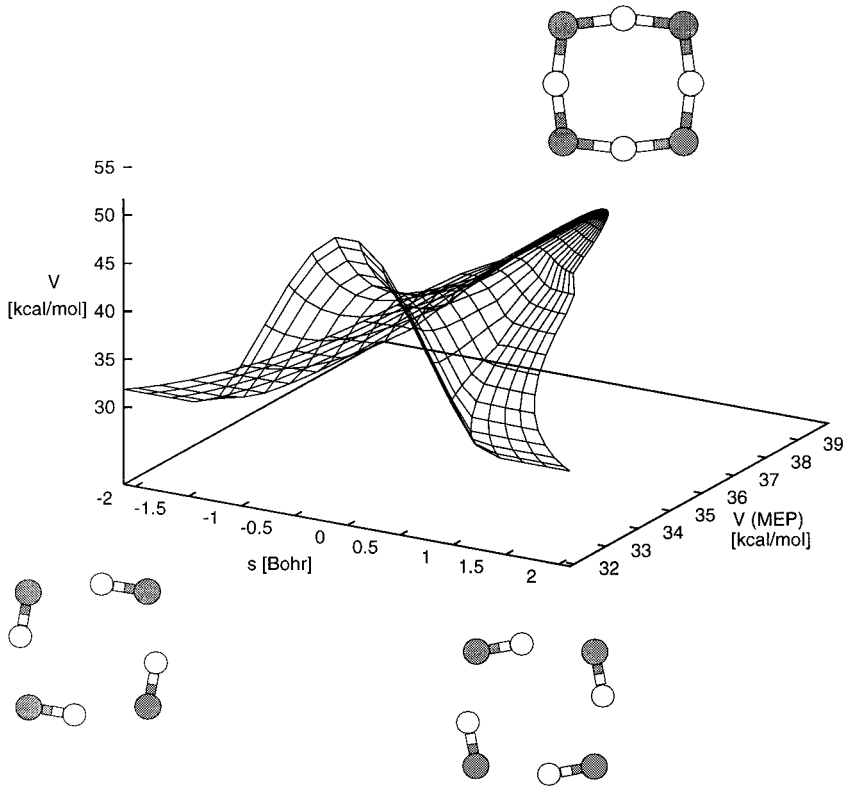

Figure 1. Part of the hypersurface used for the concerted hydrogen-transfer reaction in $(HF)_4$. The axes represent the adiabatic ground-state potential along the MEP, the reaction distance measured relative to the hypersurface dividing educts and products, and the actual adiabatic potential at a point on the hypersurface. Both minima and the transition state to concerted proton transfer are depicted near the respective positions of the hypersurface.

curvature couplings of the orthogonal normal modes.[39,40] On the other hand, the large-curvature tunneling (LCT) correction,[41−43] which corresponds to the case of a sudden, straight-line connection between the two reaction wells and therefore allows the change of the vibrational state. Because of the leaving of the vibrationally adiabatic region, a much wider part of the PES called the reaction swath[2,9,10] needs to be generated. The μOMT method uses the maximum out of the SCT and LCT calculation.[9] A typical hypersurface that arises throughout this procedure is depicted in Figure 1. The ridge of the reaction swath is defined to be the potential energy curve resulting from all points that are equidistant to both minima and can be found at $s = 0$ Bohr.

As a benchmark calculation, we computed a pure *ab initio* hypersurface at B3LYP/6-31+G(d) level of theory. This method has been shown to yield reliable results for HF clusters.[44] The slight deficiency in the barrier height to the concerted proton exchange is removed by interpolating the hypersurface according to the properties predicted by MP2/6-311++G(3df,3pd)[45] by a logarithm of ratios scheme,[46−48] shorthand MP2///B3LYP. This approach is known as direct dual-level dynamics.[9,31,49−56] For reasons of comparison we used the uninterpolated hypersurface denoted B3LYP and a semiempirical one, which was generated by adapting the PM3 parameters to fit MP2/6-311++G(3df,-3pd) results and additionally interpolated to the properties predicted by MP2/6-311++G(3df,3pd),[45] therefore called MP2/// PM3-SRP (SRP stands for specific reaction parameters) in the following. The detailed analysis of reaction paths is possible by the use of a more natural coordinate system instead of the Cartesian one. Namely, we chose the vibrational vectors (normal modes) of the TS as the basis for the description of the hypersurface. A similar approach has been called G-Matrix approach in the literature.[57−61] The tunneling splittings connected to the spectroscopically measurable energy difference of the eigenvalues of the symmetric and antisymmetric wave functions in the double well potential are estimated from the low-temperature limit of the reaction rate constant.[10,57,61−64]

3. Results

3.1. Identification of Two Crossover Temperatures. The reaction rate constants resulting from the TST treatment with additional correction for multidimensional tunneling are depicted as Arrhenius plots in Figure 2 for the exchange in $(HF)_4$ and as a simple logarithmic plot for $(HF)_5$ in Figure 3. The SCT part of the reaction dynamics calculation is about 7000 times more expensive than a single-point energy calculation, i.e., lasts about 24 days if a single-point of energy costs about 5 min. The additional calculation of a similar grid on the whole reaction swath for the LCT part would need around 5000 energy points. From a grid-convergence analysis we were able to reduce this cost to around 200 energy points.[10] The Arrhenius plots in Figure 2 together with information of the tunneling correction factors κ given in Figure 4 yield three different regimes of proton transfer and accordingly two crossover temperatures. The two linear parts of the MP2///B3LYP (LCT) Arrhenius plot meet each other at about 200 K, which is the first crossover temperature, T_{c1}. From the SCT plots T_{c1} is found between 150 K and 200 K, demonstrating that these plots can be used as good estimates. T_{c1} is easily available from experiment by just measuring the reaction rate as a function of the temperature and then analyzing the Arrhenius plot. With the analysis starting from the high-temperature regime in Figure 4, the curve starts to deviate from linearity at around 400 K, which is, therefore, the second crossover temperature, T_{c2}. It also can be identified from the numerical value of the tunneling correction factor close

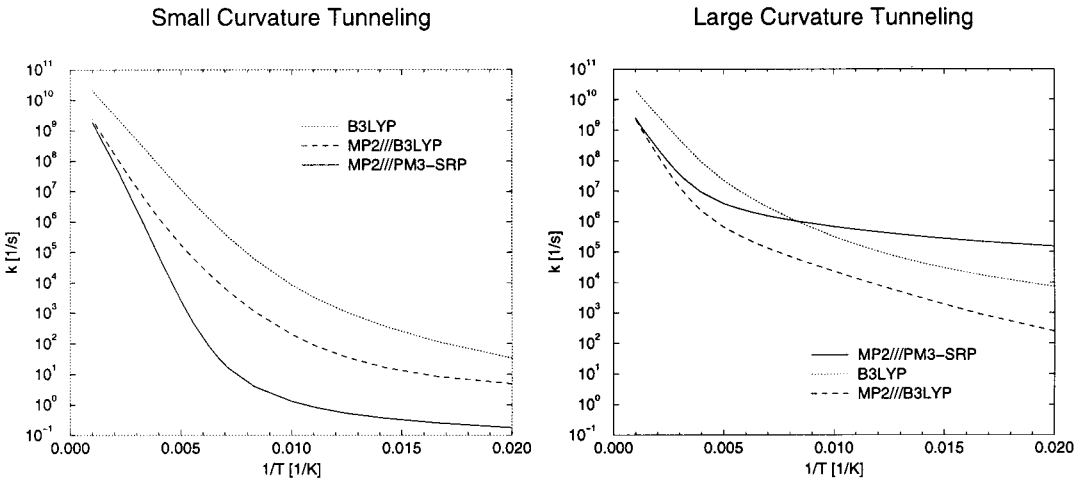

Figure 2. Arrhenius plot of reaction rate constants for the concerted multiple hydrogen-exchange reaction in planar $(HF)_4$.

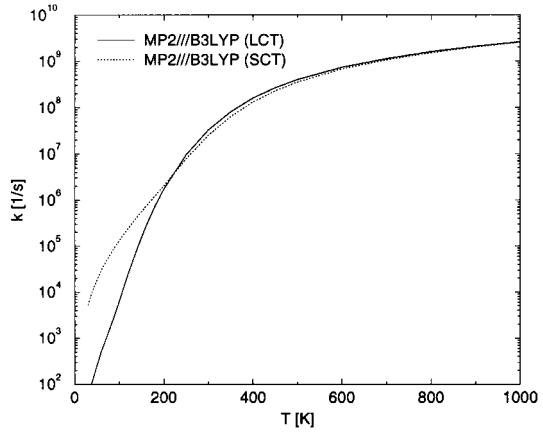

Figure 3. Reaction rate constants for the concerted multiple hydrogen-exchange reaction in planar $(HF)_5$.

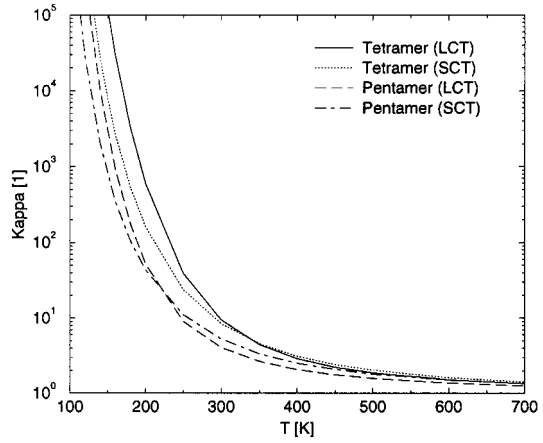

Figure 4. Correction factors κ for tunneling and corner cutting for concerted proton exchange in $(HF)_4$ and $(HF)_5$.

to 1; i.e., tunneling is unimportant. In fact, κ will be 1 only at infinitely high temperatures, as at all finite temperatures a bundle of Boltzmann-distributed paths will contribute to the reaction. The deviation of κ from the expected value can be found around 400 K, when κ is estimated from the Boltzmann distribution of reaction paths around the MEP. In theoretical models a second crossover temperature corresponding to this transition has been identified and deduced.[8,65,66] However, most experiments can only identify the lower crossover temperature, T_{c1}. The curved part in Figure 4 corresponds to the intermediate regime, where both SCT and LCT paths contribute to the reaction rate. It is this regime which contains the crossover point of tunneling corrections; i.e., κ(LCT) becomes larger than κ(SCT). For $(HF)_4$ this occurs at 350 K and for $(HF)_5$ at 220 K. The μOMT method changes from the use of SCT to the use of LCT at this point, although at any temperature both tunneling corrections are evaluated. The three different regimes will be discussed in the following in terms of stationary points, barrier height, barrier width, and potential on the swath.

3.2. Influence of the Stationary Points. The here investigated transition from one minimum to the other by concerted proton transfer is caused by only three vibrational modes as pointed out earlier.[13,45,67] The symmetric HF stretching mode causes the actual transfer, which is assisted vibrationally by the symmetric FF stretching mode and the symmetric bending mode. The dynamics thus crucially depend on a good vibrational description of the stationary points. For this reason reliable results of the hydrogen bond compression mechanism[67−72] are essential. In the transition state the FF distance in the cyclic tetramer and pentamer is reduced from about 2.50 Å to about 2.26 Å according to high-level MP2 calculations.[45] The FFH angles are close to 10° for the minima and around 5° for the TS. Mere PM3 predicts the FF distances in the $(HF)_5$ minima to be 2.60 Å, in the TS to be 2.17 Å, and the FFH angles to be 4 times larger compared to the MP2 results.[13] The PM3 reaction barrier (91.2 kcal/mol)[13] deviates strongly from the best estimate of 12.6−14.8 kcal/mol.[44,67,68,70,71] The here investigated hypersurfaces (B3LYP, PM3-SRP) all fulfill the precondition of reasonable agreement[13,44] in terms of geometries at the stationary points compared to high-level MP2 results.[67]

3.3. Influence of the Barrier Height. In principle, the barrier height ΔE enters the expression for the reaction rate constant in the exponent, i.e., $k \propto \exp(-\Delta E/RT)$. At 300 K a difference of 1 kcal/mol in the barrier therefore causes a difference in the rate constant of about a factor of 5. At 100 K the same barrier difference yields a rate error factor of about 150. On a pure B3LYP/6-31+G(d) hypersurface the barrier for the exchange in the cyclic tetramer amounts to 9.93 kcal/mol instead of 12.73 kcal/mol (MP2/6-311++G(3df,3dp)).[67] The reaction rate constant found with a hypersurface interpolated to the MP2 barrier at 300 K [k(MP2///B3LYP, LCT) = 8.2×10^6 s^{-1}] differs from the result found without interpolation [k(B3LYP, LCT) = 3.2×10^8 s^{-1}] by a factor of 40, as expected from the barrier difference. Obviously, the barrier should be known at least with chemical accuracy of 1 kcal/mol[73] to allow a prediction of the correct order of magnitude for the reaction rate at room temperature. However, in practice at 100 K this factor is only

12 instead of 10^6 as one would expect from the barrier difference of 2.8 kcal/mol [k(MP2///B3LYP, LCT) = 2.3×10^4 s^{-1}, k(B3LYP, LCT) = 2.9×10^5 s^{-1}]. The reason for the unexpected agreement of reaction rate constants between the two hypersurfaces is that at high temperatures (above 400 K) the reaction is over-barrier dominated, whereas at low temperatures (below 200 K) nonclassical tunneling dominates the reaction rate, as can also be deduced from the tunneling correction factors in Figure 4. This is affirmed by the most probable energy for direct corner cutting being 7.0 kcal/mol below the barrier maximum at 100 K in the case of the cyclic tetramer, indicating that the system avoids the transition-state region. Thus, the tunneling correction factors are increased drastically. Intermediate temperatures correspond to a mixed case where both tunneling and over-barrier trajectories prevail. The most probable tunneling energy is just 2.9 kcal/mol below the barrier top in the case of the cyclic tetramer at 300 K. At high temperatures the most probable transition between the minima occurs at the energy of the transition state. Thus, the classical rate constant estimated from the barrier height is a rather good approximation at high temperatures, even if the skew angle[7] is quite low (18° for the pentamer and 21° for the tetramer).

3.4. Influence of the Barrier Width. The comparison of the reaction rate constants between MP2///B3LYP and MP2///PM3-SRP (cf. Figure 2) shows that tunneling is slightly underestimated in the SCT limit for the exchange in $(HF)_4$. For $(HF)_5$ both SCT curves agree very well.[13] The reasons for the small discrepancy can be found in the barrier width. This width is represented by the FF stretching and symmetric bending coefficients shown in Figure 5. The normal mode corresponding to the bending has a larger coefficient along the whole MEP for MP2///PM3-SRP and is thus the main reason for an increased barrier width suppressing tunneling. The agreement of the HF and FF stretching modes is quite good, although it should be noted that pure hydrogenic motion starts at 0.6 Bohr for MP2/// B3LYP, but closer to the TS (0.4 Bohr) for MP2///PM3-SRP. This enhanced skeletal motion is another reason for the increased barrier width using MP2///PM3-SRP. These weaknesses appear again in the total reaction path curvature and thus also in the effective reduced mass for SCT (cf. Figure 6). This reduction causes the slight discrepancy to the SCT rate constants resulting from MP2///B3LYP as shown in Figure 2. Therefore, the barrier width arising from all normal modes participating actively in the transfer has to be described properly to reach agreement with experiment in the intermediate-temperature region.

3.5. Influence of the Reaction Swath. In the low-temperature plateau of the reaction rate constant the exchange rates vary by many orders of magnitude between the different hypersurfaces and tunneling corrections. As LCT yields the highest results in any case, it is clear that it constitutes the dominant mechanism. For a reliable calculation of the LCT tunneling correction the reaction swath is important, i.e., the region between the two minima away from the TS. The comparison of MP2///B3LYP (LCT) and MP2///PM3-SRP (LCT) shows a disagreement, especially below 150 K, where the reaction rates obtained from MP2///PM3-SRP (LCT) are clearly higher. In the intermediate- and high-temperature regions above 200 K, the agreement is much better, so that especially the values at room temperature for the proton-exchange rates can be considered as rather reliable and only slightly too high. When taking into account that the MP2///B3LYP (LCT) calculation is about 200 times more expensive than MP2///PM3-SRP (LCT), the agreement is astonishing. The ridge (cf. Loerting et al.[13]) explains why the

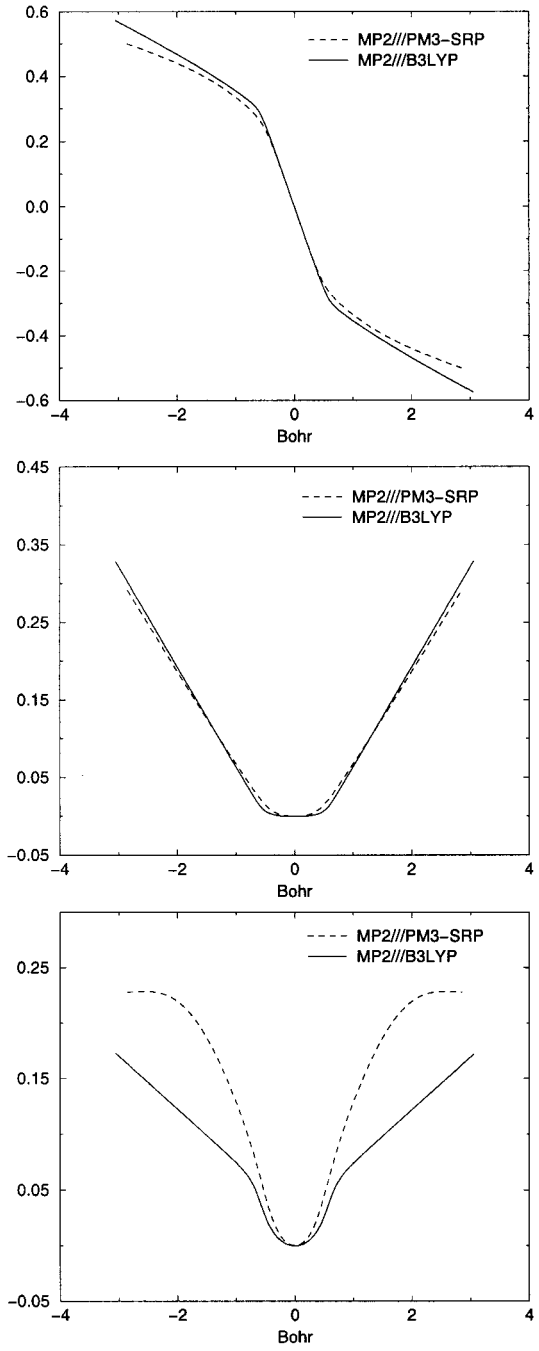

Figure 5. Basis-transformation coefficients along the MEP for the three non-zero normal modes of $(HF)_4$, namely, symmetric HF stretching (top), FF stretching (middle), and bending (bottom).

agreement is good at 300 K but not at 100 K. At higher temperatures most of the reaction paths cross near the TS. In this region the agreement of the two ridges is quite good. However, at low temperatures the system crosses far away from the TS, where the ridge gained from MP2///PM3-SRP is lower than the one gained from MP2///B3LYP. This causes the tunneling probabilities and therefore also the tunneling splittings, corresponding to proton transfer at 0 K, to grow as can be seen in Table 1. This is especially true for the proton exchange in the cyclic pentamer of HF. All splittings calculated here are clearly within the FTIR treshhold[74] of 10^{-4}—10^{-5} cm^{-1} and should be measurable if the isolation of size-selected clusters out of HF vapor or liquid HF was possible.

In summary, three different temperature regimes arise: At high temperatures (classical regime) tunneling does not play a

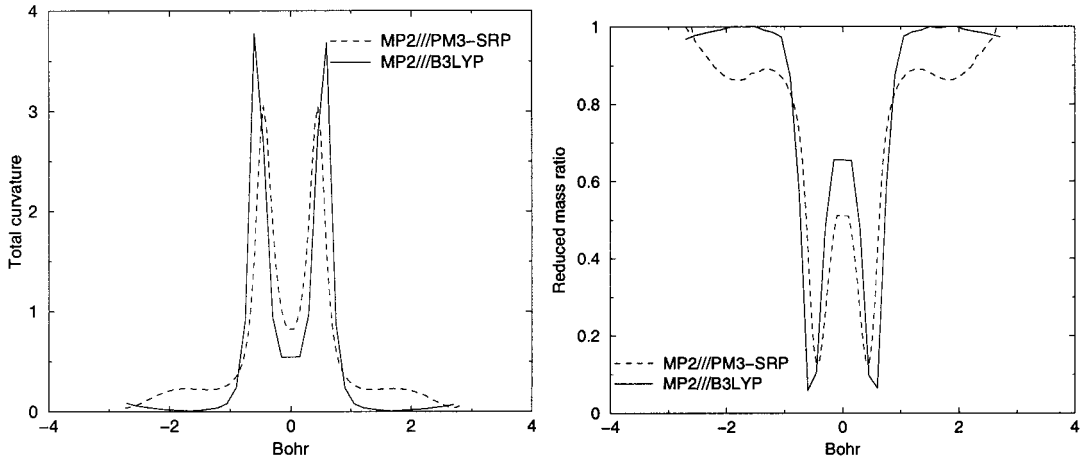

Figure 6. Total reaction path curvature (left) and effective reduced mass (right) for small curvature tunneling in $(HF)_4$.

TABLE 1: Ground-State Tunneling Splitting Estimate in cm^{-1}

	MP2///B3LYP	MP2///PM3-SRP
	LCT	
$(HF)_4$	1.0×10^{-3}	8.7×10^{-2}
$(HF)_5$	2.6×10^{-2}	4.1×10^{0}
	SCT	
$(HF)_4$	8.0×10^{-4}	4.0×10^{-4}
$(HF)_5$	8.0×10^{-3}	8.0×10^{-3}

role and all tunneling corrections vanish. At intermediate temperatures (mixed quantum-classical regime) both tunneling corrections yield similar values, indicating that the systems tunnels in the adiabatic region near the transition state (TS). At low temperatures (quantum regime) the LCT correction clearly yields the highest reaction rates, implying that tunneling occurs far away from the TS in the nonadiabatic region. Tunneling splittings are, therefore, caused only by straight-line LCT paths.

4. Conclusions

We have presented an analysis of how proton transfer takes place, depending on the temperature. The results imply strategies for reproducing experimental reaction rates and tunneling splittings by computational models. The calculation of reaction rate constants can only be reliable if certain quality requirements on the underlying PESs are fulfilled. These requirements can be separated in three categories, depending on the temperature. At high temperatures above 400 K (in the case of concerted proton exchange in cyclic oligomers of HF), at which the tunneling corrections vanish, the knowledge of the reaction barrier to chemical accuracy[73] is needed. At intermediate temperatures between 200 and 400 K (between the two crossover temperatures) the barrier width needs to be known and at least an adiabatic tunneling model like SCT must be used. Nevertheless, the LCT reaction rate constants are essentially identical to the SCT constants in this intermediate region. At low temperatures below 200 K the system avoids reaching the transition state by directly crossing the reaction swath. Therefore, the LCT correction provides by far the best estimate for the experimental rate constants. In further consequence this is also valid for the experimentally observable tunneling splittings related to the 0 K limit of the coherent reaction rate. Therefore, for LCT a proper description of the reaction swath is very important. Especially, a good description of the high-energy region of the ridge of the reaction swath is essential to allow direct comparison with experimental data.

The effect of two different crossover temperatures manifests itself already in simple two-dimensional prototype models of vibration-assisted tunneling,[8,65,66] describing proton transfer by just (q, Q) coordinates. The q motion corresponds to the actual proton transfer and the Q motion corresponds to rearrangement of the heavy atoms. On the one hand, at low temperatures the slow Q motion is frozen and the q motion dominates the reaction by tunneling. On the other hand, at high temperatures the Q motion is fast, so that the q transition occurs predominantly at the transition state, where the barrier is lowest. At intermediate temperatures both coordinates are of similar importance, yielding the mixed behavior.

We believe, therefore, that the finding of three different temperature regimes for proton transfer and consequently three different quality requirements on dynamical calculations is valid for most systems exhibiting proton transfer. The direct relation between crossover temperatures and these requirements provides a basis for a method expanding the capabilities of the well-established μOMT method, which lacks such a direct comparison and which does not optimize the use of computer resources. It is especially possible to judge from the analysis of the adiabatic tunneling correction factors (SCT) whether it is necessary to include nonadibatic reaction paths (LCT) or not at a certain temperature. One knows, therefore, what kind of region on the potential energy surface is traversed, i.e., where accurate calculations are required. In this sense this study provides a basis for the calculation of proton-transfer data in various flourishing fields of chemistry like atmospheric chemistry,[75−85] DNA mutation,[86−88] enzymes,[89−100] or in the field of explaining the extraneously high conductivity in water.[101−107] However, it is clear that the values of the crossover temperatures for these systems can be very different.

5. Acknowledgment

The authors are grateful to Martin A. Suhm for suggesting investigation of the use of B3LYP with small basis sets as a low-level method for the calculation of rate constants. Thomas Loerting acknowledges financial support by the Austrian Academy of Sciences.

References and Notes

(1) Dunning, T. H., Jr.; Harding, L. B.; Wagner, A. F.; Schatz, G. C.; Bowman, J. M. *Science* **1988**, *240*, 453−459.

(2) Truhlar, D. G.; Gordon, M. S. *Science* **1990**, *249*, 491−498.

(3) Angell, A. *Nature* **1998**, *393*, 521−524.

(4) Sastry, S.; Debenedetti, P. G.; Stillinger, F. H. *Nature* **1998**, *393*, 554−557.

(5) Wales, D. J.; Miller, M. A.; Walsh, T. R. *Nature* **1998**, *394*, 758−760.

(6) Tucker, S. C.; Truhlar, D. G. Dynamical Formulation of Transition State Theory: Variational Transition States and Semiclassical Tunneling. In *New Theoretical Concepts for Understanding Organic Reactions*; Bertrán, J., Csizmadia, I. G., Eds.; NATO ASI Series C 267; Kluwer: Dordrecht, The Netherlands, 1989; pp 291−346.

(7) Truhlar, D. G.; Isaacson, A. D.; Garrett, B. C. Generalized Transition State Theory. In *Theory of Chemical Reaction Dynamics*; Baer, M., Ed.; CRC Press: Boca Raton, FL, 1985; pp 65−137.

(8) Benderskii, V. A.; Makarov, D. E.; Wight, C. A. *Chemical Dynamics at Low Temperatures*; Advances in Chemical Physics; John Wiley & Sons, Inc.: New York, 1994; Vol. 88.

(9) Liu, Y.-P.; Lu, D.-h.; Gonzalez-Lafont, A.; Truhlar, D. G.; Garrett, B. C. *J. Am. Chem. Soc.* **1993**, *115*, 7806−7817.

(10) Loerting, T.; Liedl, K. R.; Rode, B. M. *J. Chem. Phys.* **1998**, *109*, 2672−2679.

(11) Eyring, H. *J. Chem. Phys.* **1935**, *3*, 107−115.

(12) Glasstone, S.; Laidler, K.; Eyring, H. *The Theory of Rate Processes*; McGraw-Hill: New York, 1941.

(13) Loerting, T.; Liedl, K. R.; Rode, B. M. *J. Am. Chem. Soc*. **1998**, *120*, 404−412.

(14) Truhlar, D. G.; Hase, W. L.; Hynes, J. T. *J. Phys. Chem.* **1983**, *87*, 2664−2682.

(15) Laidler, K. J.; King, M. C. *J. Phys. Chem.* **1983**, *87*, 2657−2664.

(16) Truhlar, D. G.; Garrett, B. C. *Ann. Rev. Phys. Chem.* **1984**, *35*, 159−189.

(17) Kreevoy, M. M.; Truhlar, D. G. Transition State Theory. In *Investigation of Rates and Mechanisms of Reactions*; Bernasconi, C. F., Ed.; John Wiley & Sons, Inc.: New York, 1986; pp 13−95.

(18) Garrett, B. C.; Melius, C. F. In *Theoretical and Computational Models for Organic Chemistry*; Formosinho, S. J., et al., Eds.; NATO ASI Series C 339; Kluwer Academic: The Netherlands, 1991; pp 35−54.

(19) Truhlar, D. G.; Garrett, B. C.; Klippenstein, S. J. *J. Phys. Chem.* **1996**, *100*, 12771−12800.

(20) Guthrie, J. P. *J. Am. Chem. Soc.* **1996**, *118*, 12878−12885.

(21) Kay, K. G. *J. Chem. Phys.* **1997**, *107*, 2313−2328.

(22) Guo, Y.; Li, S.; Thompson, D. L. *J. Chem. Phys.* **1997**, *107*, 2853−2858.

(23) Zhu, C.; Nakamura, H. *J. Chem. Phys.* **1997**, *107*, 7839−7848.

(24) Huo, S.; Straub, J. E. *J. Chem. Phys.* **1997**, *107*, 5000−5006.

(25) Villa, J.; Truhlar, D. G. *Theor. Chem. Acc.* **1997**, *97*, 317−323.

(26) Makarov, D. E.; Metiu, H. *J. Chem. Phys.* **1997**, *107*, 7787−7799.

(27) Miller, W. H. *J. Phys. Chem. A* **1998**, *102*, 793−806.

(28) Chuang, Y.-Y.; Truhlar, D. G. *J. Phys. Chem. A* **1998**, *102*, 242−247.

(29) Topaler, M. S.; Allison, T. C.; Schwenke, D. W.; Truhlar, D. G. *J. Phys. Chem. A* **1998**, *102*, 1666−1673.

(30) Corchado, J. C.; Coitiño, E. L.; Chuang, Y.-Y.; Fast, P. L.; Truhlar, D. G. *J. Phys. Chem. A* **1998**, *102*, 2424−2438.

(31) Fernández-Ramos, A.; Rodríguez-Otero, J.; Ríos, M. A. *J. Phys. Chem. A* **1998**, *102*, 2954−2961.

(32) Dellago, C.; Bolhuis, P. G.; Csajka, F. S.; Chandler, D. *J. Chem. Phys.* **1998**, *108*, 1964−1977.

(33) Chuang, Y.-Y.; Corchado, J. C.; Fast, P. L.; Villá, J.; Coitiño, E. L.; Hu, W.-P.; Liu, Y.-P.; Lynch, G. C.; Nguyen, K. A.; Jackels, C. F.; Gu, M. Z.; Rossi, I.; Clayton, S.; Melissas, V. S.; Steckler, R.; Garrett, B. C.; Isaacson, A. D.; Truhlar, D. G. *POLYRATE-version 8.0*; University of Minnesota: Minneapolis, MN, 1998.

(34) Frisch, M. J.; Trucks, G. W.; Schlegel, H. B.; Scuseria, G. E.; Robb, M. A.; Cheeseman, J. R.; Zakrzewski, V. G.; Montgomery, J. A.; Stratmann, R. E.; Burant, J. C.; Dapprich, S.; Millam, J. M.; Daniels, A. D.; Kudin, K. N.; Strain, M. C.; Farkas, O.; Tomasi, J.; Barone, V.; Cossi, M.; Cammi, R.; Mennucci, B.; Pomelli, C.; Adamo, C.; Clifford, S.; Ochterski, J.; Petersson, G. A.; Ayala, P. Y.; Cui, Q.; Morokuma, K.; Malick, D. K.; Rabuck, A. D.; Raghavachari, K.; Foresman, J. B.; Cioslowski, J.; Ortiz, J. V.; Stefanov, B. B.; Liu, G.; Liashenko, A.; Piskorz, P.; Komaromi, I.; Gomperts, R.; Martin, R. L.; Fox, D. J.; Keith, T.; Al-Laham, M. A.; Peng, C. Y.; Nanayakkara, A.; Gonzalez, C.; Challacombe, M.; Gill, P. M. W.; Johnson, B. G.; Chen, W.; Wong, M. W.; Andres, J. L.; Head-Gordon, M.; Replogle, E. S.; Pople, J. A. *Gaussian 98*, Revision A.4; Gaussian, Inc.: Pittsburgh, PA, 1998.

(35) Corchado, J. C.; Coitiño, E. L.; Chuang, Y.-Y.; Truhlar, D. G. *Gaussrate8.0*; University of Minnesota: Minneapolis, MN, 1998.

(36) Page, M.; McIver, J. W., Jr. *J. Chem. Phys.* **1988**, *88*, 922−935.

(37) Melissas, V. S.; Truhlar, D. G.; Garrett, B. C. *J. Chem. Phys.* **1992**, *96*, 5758−5772.

(38) Marcus, R. A.; Coltrin, M. E. *J. Chem. Phys.* **1977**, *67*, 2609.

(39) Skodje, R. T.; Truhlar, D. G.; Garrett, B. C. *J. Phys. Chem.* **1981**, *85*, 3019−3023.

(40) Skodje, R. T.; Truhlar, D. G.; Garrett, B. C. *J. Chem. Phys.* **1982**, *77*, 5955−5976.

(41) Garrett, B. C.; Truhlar, D. G. *J. Chem. Phys.* **1983**, *79*, 4931−4938.

(42) Garrett, B. C.; Joseph, T.; Truong, T. N.; Truhlar, D. G. *Chem. Phys.* **1989**, *136*, 271−283.

(43) Lynch, G. C.; Truhlar, D. G.; Garrett, B. C. *J. Chem. Phys.* **1989**, *90*, 3102−3109.

(44) Märker, C.; Schleyer, P. v. R.; Liedl, K. R.; Ha, T.-K.; Quack, M.; Suhm, M. A. *J. Comput. Chem.* **1997**, *18*, 1695−1719.

(45) Liedl, K. R.; Sekusak, S.; Kroemer, R. T.; Rode, B. M. *J. Phys. Chem. A* **1997**, *101*, 4707−4716.

(46) Hu, W.-P.; Liu, Y.-P.; Truhlar, D. G. *J. Chem. Soc., Faraday Trans.* **1994**, *90*, 1715−1725.

(47) Nguyen, K. A.; Rossi, I.; Truhlar, D. G. *J. Chem. Phys.* **1995**, *103*, 5522−5530.

(48) Chuang, Y.-Y.; Truhlar, D. G. *J. Phys. Chem. A* **1997**, *101*, 3808−3814.

(49) Baldridge, K. K.; Gordon, M. S.; Steckler, R.; Truhlar, D. G. *J. Phys. Chem.* **1989**, *93*, 5107−5119.

(50) Truhlar, D. G. Direct Dynamics Method for the Calculation of Reaction Rates. In *The Reaction Path in Chemistry: Current Approaches and Perspectives*; Heidrich, D., Ed.; Kluwer: Dordrecht, 1995; pp 229−255.

(51) Corchado, J. C.; Espinosa-Garcia, J.; Hu, W.-P.; Rossi, I.; Truhlar, D. G. *J. Phys. Chem.* **1995**, *99*, 687−694.

(52) Kim, Y. *J. Am. Chem. Soc.* **1996**, *118*, 1522−1528.

(53) Rosenman, E.; McKee, M. L. *J. Am. Chem. Soc.* **1997**, *119*, 9033−9038.

(54) Roberto-Neto, O.; Coitiño, E. L.; Truhlar, D. G. *J. Phys. Chem. A* **1998**, *102*, 4568−4578.

(55) Corchado, J. C.; Espinosa-García, J.; Roberto-Neto, O.; Chuang, Y.-Y.; Truhlar, D. G. *J. Phys. Chem. A* **1998**, *102*, 4899−4910.

(56) Fernández-Ramos, A.; Martínez-Núñez, E.; Ríos, M. A.; Rodríguez-Otero, J.; Vázquez, S. A.; Estévez, C. M. *J. Am. Chem. Soc.* **1998**, *120*, 7594−7601.

(57) Smedarchina, Z.; Siebrand, W.; Zgierski, M. Z. *J. Chem. Phys.* **1995**, *103*, 5326−5334.

(58) Smedarchina, Z.; Siebrand, W.; Zgierski, M. Z. *J. Chem. Phys.* **1996**, *104*, 1203−1212.

(59) Smedarchina, Z.; Fernandez-Ramos, A.; Rios, M. A. *J. Chem. Phys.* **1997**, *106*, 3956−3964.

(60) Smedarchina, Z.; Zgierski, M. Z.; Siebrand, W.; Kozlowski, P. M. *J. Chem. Phys.* **1998**, *109*, 1014−1024.

(61) Fernández-Ramos, A.; Smedarchina, Z.; Zgierski, M. Z.; Siebrand, W. *J. Chem. Phys.* **1998**, *109*, 1004−1013.

(62) Smedarchina, Z.; Caminati, W.; Zerbetto, F. *Chem. Phys. Lett.* **1995**, *237*, 279−285.

(63) Benderskii, V. A.; Vetoshkin, E. V.; Grebenshchikov, S. Y.; von Laue, L.; Trommsdorff, H. P. *Chem. Phys.* **1997**, *219*, 119−142.

(64) Loerting, T.; Liedl, K. R. *J. Am. Chem. Soc.* **1998**, *120*, 12595−12600.

(65) Johnston, H. S.; Rapp, D. *J. Am. Chem. Soc.* **1961**, *83*, 1−9.

(66) Dakhnovskii, Y. I.; Semenov, M. B. *J. Chem. Phys.* **1989**, *91*, 7606−7611.

(67) Liedl, K. R.; Kroemer, R. T.; Rode, B. M. *Chem. Phys. Lett.* **1995**, *246*, 455−462.

(68) Karpfen, A. *Int. J. Quantum Chem., Quantum Chem. Symp.* **1990**, *24*, 129−140.

(69) Karpfen, A.; Yanovitskii, O. *J. Mol. Struct. (Theochem)* **1994**, *314*, 211−227.

(70) Quack, M.; Suhm, M. A. Potential Energy Hypersurfaces For Hydrogen Bonded Clusters $(HF)_N$. In *Conceptual Perspectives in Quantum Chemistry*; Conceptual Trends in Quantum Chemistry; Kluwer Publishing Co.: Dordrecht, 1997; Vol. 3, pp 417−467.

(71) Klopper, W.; Quack, M.; Suhm, M. A. *Mol. Phys.* **1998**, *94*, 105−119.

(72) Karpfen, A. Case Studies on Cooperativity in Hydrogen Bonded Clusters and Polymers: Neutral Chain-like and Cyclic Clusters of Hydrogen Fluoride and Hydrogen Cyanide and Charged Defects on Chain-like Hydrogen Fluoride Oligomers. In *Molecular Interactions—From van der Waals to Strongly Bound Complexes*; Scheiner, S., Ed.; Wiley: Chichester, UK, 1997; pp 265−296.

(73) Boys, S. F.; Bernardi, F. *Mol. Phys.* **1970**, *19*, 553−566.

(74) Pugliano, N.; Saykally, R. J. *Science* **1992**, *257*, 1937−1940.

(75) Chen, T. S.; Moore Plummer, P. L. *J. Phys. Chem.* **1985**, *89*, 3689−3693.

(76) Wang, X.; Jin, Y. G.; Suto, M.; Lee, L. C. *J. Chem. Phys.* **1988**, *89*, 4853−4860.

(77) Hofmann, M.; Schleyer, P. v. R. *J. Am. Chem. Soc.* **1994**, *116*, 4947−4952.

(78) Morokuma, K.; Muguruma, C. *J. Am. Chem. Soc.* **1994**, *116*, 10316−10317.

(79) Kolb, C. E.; Jayne, J. T.; Worsnop, D. R.; Molina, M. J.; Meads, R. F.; Viggiano, A. A. *J. Am. Chem. Soc.* **1994**, *116*, 10314−10315.

(80) Li, W.-K.; McKee, M. L. *J. Phys. Chem. A* **1997**, *101*, 9778−9782.

(81) Arstila, H.; Laasonen, K.; Laaksonen, A. *J. Chem. Phys.* **1998**, *108*, 1031−1039.
(82) Bishenden, E.; Donaldson, D. J. *J. Phys. Chem. A* **1998**, *102*, 4638−4642.
(83) Bianco, R.; Hynes, J. T. *J. Phys. Chem. A* **1998**, *102*, 309−314.
(84) Bianco, R.; Gertner, B. J.; Hynes, J. T. *Ber. Bunsen.-Ges. Phys. Chem.* **1998**, *102*, 518−526.
(85) Xu, S. C.; Zhao, X. S. *J. Phys. Chem. A* **1999**, *103*, 2100−2106.
(86) Topal, M. D.; Fresco, J. R. *Nature* **1976**, *263*, 285.
(87) Sänger, W. *Principles of Nucleic Acid Structure*; Springer: New York, 1984.
(88) Florián, J.; Leszczyński, J. *J. Am. Chem. Soc.* **1996**, *118*, 3010−3017.
(89) Pocker, Y.; Janjić, N. *J. Am. Chem. Soc.* **1989**, *111*, 731−733.
(90) Merz, K. M., Jr.; Hoffmann, R.; Dewar, M. J. S. *J. Am. Chem. Soc.* **1989**, *111*, 5636−5649.
(91) Kadenbach, B. *Angew. Chem., Int. Ed. Engl.* **1996**, *34*, 2635−2637.
(92) Lu, D.; Voth, G. A. *J. Am. Chem. Soc.* **1998**, *120*, 4006−4014.
(93) Gennis, R. B. *Science* **1998**, *280*, 1712−1713.
(94) Yoshikawa, S.; Shinzawa-Itoh, K.; Nakashima, R.; Yaono, R.; Yamashita, E.; Inoue, N.; Yao, M.; Fei, M. J.; Libeu, C. P.; Mizushima, T.; Yamaguchi, H.; Tomizaki, T.; Tsukihara, T. *Science* **1998**, *280*, 1723−1729.
(95) Hucho, F. *Angew. Chem., Int. Ed.* **1998**, *37*, 1518−1519.
(96) Gai, F.; Hasson, K. C.; McDonald, J. C.; Anfinrud, P. A. *Science* **1998**, *279*, 1886−1891.
(97) Luecke, H.; Richter, H.-T.; Lanyi, J. K. *Science* **1998**, *280*, 1934−1937.
(98) Guo, H.; Salahub, D. R. *Angew. Chem., Int. Ed.* **1998**, *37*, 2985−2990.
(99) Toba, S.; Colombo, G.; Merz, K. M., Jr. *J. Am. Chem. Soc.* **1999**, *121*, 2290−2302.
(100) Denisov, V. P.; Jonsson, B.-H.; Halle, B. *J. Am. Chem. Soc.* **1999**, *121*, 2327−2328.
(101) Pomés, R.; Roux, B. *Chem. Phys. Lett.* **1995**, *234*, 416−424.
(102) Schmidt, R. G.; Brickmann, J. *Ber. Bunsen.-Ges. Phys. Chem.* **1997**, *101*, 1816−1827.
(103) Tuckerman, M. E.; Marx, D.; Klein, M. L.; Parrinello, M. *Science* **1997**, *275*, 817−820.
(104) Pomés, R.; Roux, B. *Biophys. J.* **1998**, *75*, 33−40.
(105) Marx, D.; Tuckerman, M. E.; Hutter, J.; Parrinello, M. *Nature* **1999**, *397*, 601−604.
(106) Hynes, J. T. *Nature* **1999**, *397*, 565−566.
(107) Decornez, H.; Drukker, K.; Hammes-Schiffer, S. *J. Phys. Chem. A* **1999**, *103*, 2891−2898.